MATEMATIKA: MJIAM, Special Issue, December 2019, 15–32

Numerical Calculation of Two-Dimensional Subsea Cable Tension Problem Using Minimization Approach

[1]Nur Azira Jasman*, [2]Nur Adlin Lina Normisyidi, [3]Yeak Sue Hoe, [4]Ahmad Razin Zainal Abidin and [5]Mohd Ridza Mohd Haniffah

[1,3]Department of Mathematical Sciences, Universiti Teknologi Malaysia
81310 UTM Johor Bahru, Malaysia

[2,4]Department of Structure and Materials, Universiti Teknologi Malaysia
81310 UTM Johor Bahru, Malaysia

[5]Department of Water and Environmental Engineering, Universiti Teknologi Malaysia
81310 UTM Johor Bahru, Malaysia

*Corresponding author: nurazirajasman@gmail.com

Article history
Received: 10 November 2019
Received in revised form: 21 November 2019
Accepted: 23 December 2019
Published online: 31 December 2019

Abstract Subsea cable laying is a risky and challenging operation faced by engineers, due to many uncertainties arise during the operation. In order to ensure that subsea cables are laid out diligently, the analysis of subsea cable tension during the laying operation is crucial. This study focuses on the fatigue failure of cables that will cause large hang-off loads based on catenary configuration after laying operation. The presented problem was addressed using mathematical modelling with consideration for a number of defining parameters, which include external forces such as current velocity and design parameters such as cable diameter. There were two types of subsea cable tension analyses studied: tensional analysis of catenary configurations and tensional analysis of lazy wave configurations. The latter involved a buoyancy module that was incorporated in the current catenary configuration that reduced subsea cable tension and enhanced subsea cable lifespan. Both analyses were solved using minimization through the gradient-based approach concerning on the tensional analysis of the subsea cable in different configurations. Lazy wave configurations were shown to successfully reduce cable tension, especially at the hang-off section.

Keywords Two-dimensional, Steady state problem, Catenary configuration, Lazy wave configuration, Minimization with gradient-based approach.

Mathematics Subject Classification 65D99, 65K05

1 Introduction

Subsea cable systems have been extensively used worldwide since the mid-19th century. Ever since subsea cable has played an important role in providing communications due to

their massive capacity, great reliability, and excellent communication quality. The rapid of development of telecommunication systems has led to the exploitation of ocean environment resources and the intensive deployment of subsea cables. During the subsea cable deployment process, any incorrect manipulation scan cause unrepairable subsea cable damage. Therefore, the tension analysis of subsea cables has been explored by researcher over the past few decades.

Attention have been paid for the last few decades to theoretical studies about the static and dynamic responses of subsea cables during the deployment process. Zajac [1] was the first to develop a steady state theory for subsea cables in a typical deployment process in which the model assumed as a straight line and excluded the effect of transient motions. Followed from the theory developed by Zajac [1], many studies have considered different analysis approaches for both static and dynamic subsea cable response [2-3]. After Zajac [1], Patel and Vaz [4] extended the steady state model into a two-dimensional model of transient subsea cable behavior in which the developed model was used to analyze cable top tension, required pay out rate as a function of time, and cable configuration whenever a ship accelerates or decelerates. The two-dimensional model was then extended into a three-dimensional model that considered the sheared currents effect, subsea cable elastic deformation, and vessel speed during the laying process using the conventional finite element method and Runge-Kutta technique [5-10].

The numerical and experimental dynamic behavior results of subsea cables have been a great interest to the subsea cable design process. A comparison of the numerical and experimental results of this problem have been discussed in past studies in [11-14] in which subsea cable bending stiffness was calculated using the cable shape to determine where the cable experienced the greatest stress and thrust from the laying ship. A recent study by Han *et al.* [15] established a mathematical model in which the initial-boundary value problem was addressed using a Partial Differential Equation (PDE). These mathematical models have been used to describe the three-dimensional motion of subsea cables being laid onto the seabed of varying depths.

Subsea cable installation is an extremely important lifetime process that requires very precise control. One of the challenges faced during subsea cable deployment is slack formation as stated by Abidin *et al.* [16]. Slack formed during the subsea cable laying process increases the possibility of the cable being laid too long for planed route,causing a buckling issue at the touchdown point (TDP). According to Wang *et al.* [17], the configuration and performance of subsea cables are essential to subsea cable installation. A free hanging subsea cable hangs from a floating production vessel to the seabed, forming a catenary shape has a lower manufacturing cost and good ability to resist high temperature. However, this kind of configuration may face buckling issues at the touchdown zone. Variations in catenary configurations were developed considering the existence of buoyancy modules, which are a logical extension of the catenary shape. These new variations in catenary configurations were modeled by installing buoyancy modules into subsea cables at a certain part to eliminate partial tension. According to Wang and Duan [18], buoyancy modules equipped onto subsea cables tend to decouple catenary configurations from surface dynamics in the touchdown region, which ensures that the strength, fatigue performance, and platform payload of the cable are within acceptable limits.

In summary, most studies have mainly focused on subsea cables without buoyancy modules to allow for simple and easy subsea cable installation. Hence, this study extends the formulated mathematical model by including buoyancy modules to provide insight into subsea cables catenary configurations, which are very sensitive to fatigue and have a high top tension. The implementation of buoyancy modules onto subsea cables in past studies only focused on the

pipeline itself to show the buoyancy modules ability to reduce tension along the pipeline. Thus, this study was conducted to provide insight into the work ability of buoyancy modules on subsea cables as both subsea cables and pipelines are slender structures subject to the similar accidental impact loads with different local damage mechanisms due to the discrepancies in cable diameter, structural configuration, and flexural rigidity.

The problem considered in this study considered subsea cables in the (1) catenary configuration, and (2) lazy wave configuration. The study theory was formulated and used to solve problems related to subsea cable tension analysis in engineering applications. In this study, subsea cable tension analysis was based on the following assumptions:

- Continuity: Subsea cables were considered continuous in terms of tension and force analysis
- Flexibility: Bending stiffness was neglected, and bending was only considered except momentarily at the sea surface node of the top boundary condition
- The subsea cable was assumed to be fully immersed in sea water
- The drag coefficient (C_D), lift coefficient (C_L), water density (ρ_w), and cable density (ρ_c) were considered constant.

2 Theoretical Model

The first model formulated in this paper was based on subsea cables in catenary configurations. The aim of this model was to analyze the position of maximum tension on the subsea cable during its practical installation in a steady state condition. This model was further enhanced by the installation of a buoyancy module on certain parts of the subsea cable to create a lazy wave configuration.

2.1 Equilibrium Equations for the Subsea Cable in Water

The model formulated in this study was based on the Cartesian coordinate system. This paper established a two-dimensional subsea cable mathematical model that considered ocean environmental effects such as lift force, drag force, and ocean current for steady state cases. When a subsea cable is laid from the floating production vessel to the TDP, the components that contribute to the tensional forces (T) along the subsea cable can be described as:

- Gravity force ($W\Delta s$), which is due to subsea cable self-weight
- Buoyancy force (B), which is equal to the weight of its displaced fluid
- Drag force (D), which is the force a flowing fluid exerts on a body in the flow direction
- Lift force (L), which is the force a flowing fluid exerts on a body in the normal flow direction

Considering a cable length as an infinitesimal element, with a leftward Δs and water flow direction, the possible forces acting on a subsea cable in water is illustrated in Figure 1.

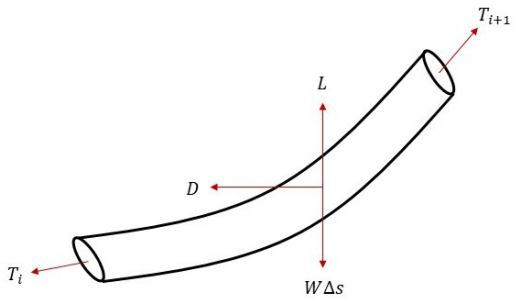

Figure 1: Forces Acting on The Subsea Cable in Water Per Element.

2.2 Mathematical Model of Subsea Cables in Catenary Configurations

Catenary shape of subsea cables can be described as a free hanging subsea cable without a buoyancy module hanging from a floating production vessel to the seabed. It has become a popular configuration for the deployment of subsea cables near platforms as it is a low cost alternative to subsea cable design.

In steady state conditions, the subsea cable is considered to be laid onto the seabed and the last point of the cable touching the seabed is known as the touchdown point (TDP), which is fixed in place. The TDP is the initial point from which the length of the subsea cable is measured to the floating production vessel. The parameter, s (arc length) was introduced to denote the length of the subsea cable. The study model does not consider the sea surface effect (wave) on the subsea cable.

Based on the Cartesian coordinate system, the cable laying ship starts at origin, o. The ship sails and lays the subsea cable from point P along the prescribed lines. The arc length, s is introduced to denote the length of the cable from point P to any point until the desired cable configuration is achieved. Figure 2 illustrate a subsea cable in a catenary configuration. Based on Figure 2, V_x is the velocity of water (current velocity) and H is the water depth.

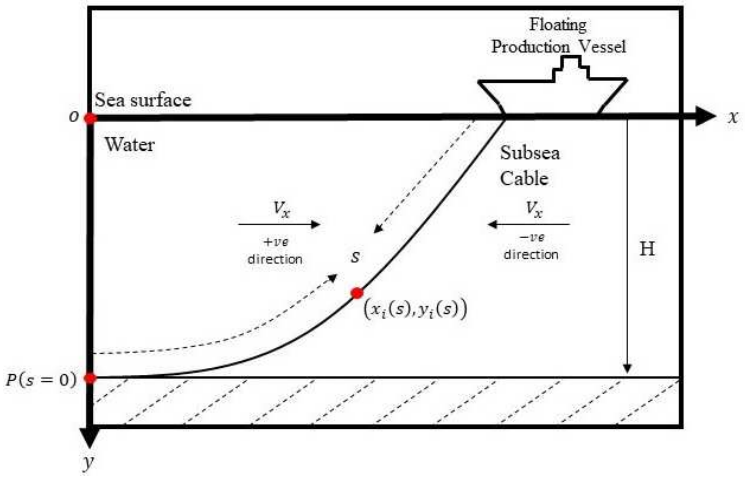

Figure 2: Illustration of Subsea Cable in Catenary Configuration.

The two-dimensional subsea cable steady state model was derived based on some physical and mechanical subsea cable laws. This study's notations are described as follows:

r	-	The radius of subsea cable, where $d = 2r$ is the diameter of subsea cable.
g	-	Gravitational acceleration.
W	-	Self-weight of a cable per unit length in water.
$T_{x_i}(s)$	-	Tension force at i^{th} point in the x-direction.
$T_{y_i}(s)$	-	Tension force at i^{th} point in the y-direction.
ρ_c	-	Density of subsea cable.
ρ_w	-	Density of seawater.
$\rho g \Delta s$	-	Gravity of cable segment Δs, $\rho = \pi r^2 \rho_c$.
$\rho_o g \Delta s$	-	Buoyancy of cable segment Δs, $\rho_o = \pi r^2 \rho_w$.
D_x	-	Drag force of seawater in the x-direction.
D_y	-	Drag force of seawater in the y-direction.
L_x	-	Lift force of seawater in the x-direction.
L_y	-	Drag force of seawater in the y-direction.

Generally, the drag force, D and lift force, L were obtained when the upstream velocity (relative to body) of fluid, V and fluid density, ρ_f were measured using flow over body using Equation (1) and (2), respectively.

$$D = C_D \frac{\rho_f}{2} V^2 A_p \tag{1}$$

$$L = C_L \frac{\rho_f}{2} V^2 A \tag{2}$$

C_D in Equation (1) denote the total drag coefficient while C_L in Equation (2) is the total lift force. A_p is the frontal area which means the projected area seen by a person looking toward the object from a direction parallel to the upstream velocity V and variable A is the planform area seen by a person looking toward the object from a direction normal to the upstream velocity V.

In this study, the water velocity along the y-direction was neglected as it is very small in the ocean where $v_y(x, y) = 0$. Water velocity along the x-direction was written as $v_x = V_x(x, y)\vec{m} = (U_x, U_y)$ was the velocity of the cable segment relative to the water while $\vec{\ell}$ was a vector of $\vec{\ell} = (\Delta x, \Delta y)$. The drag and lift force in the x-direction and y-direction were defined using Equation (3) and (4) respectively considering the vector of $\vec{m}$ and $\vec{\ell}$.

$$\begin{aligned} D_{x_i} &= -K_D U_{x_i} \left| \vec{\ell}_i \times \vec{m}_i \right| \\ D_{y_i} &= -K_D U_{y_i} \left| \vec{\ell}_i \times \vec{m}_i \right| \end{aligned} \tag{3}$$

$$\begin{aligned} L_{x_i} &= K_L U \left| \vec{\ell}_i \cdot \vec{m}_i \right| \frac{E(1,0)}{\sum} sgn\left(\vec{\ell}_i \cdot \vec{m}_i \right) \\ L_{y_i} &= K_L U \left| \vec{\ell}_i \cdot \vec{m}_i \right| \frac{E(0,1)}{\sum} sgn\left(\vec{\ell}_i \cdot \vec{m}_i \right) \end{aligned} \tag{4}$$

where the K_D and and K_L used in Equations (3) and (4) were drag and lift coefficient defined using Equations (5) and (6) respectively, while parameter $E\,(a,b)$ was defined using Equation (7)

$$K_D = C_D \frac{\rho_w}{2} d \tag{5}$$

$$K_L = C_L \frac{\rho_w}{2} d \tag{6}$$

$$E\,(a,b)\left(U^2 - aU_{x_i}^2 - bU_{y_i}^2\right)\left(a\frac{\partial x}{\partial s} + b\frac{\partial y}{\partial s}\right) - \left[(1-a)\,U_{x_i}\frac{\partial x}{\partial s} + (1-b)\,U_{y_i}\frac{\partial y}{\partial s}\right](aU_{x_i} + bU_{y_i}) \tag{7}$$

The direction of the drag and lift forces with respect to the direction of the upstream velocity, V is illustrated in Figure 3.

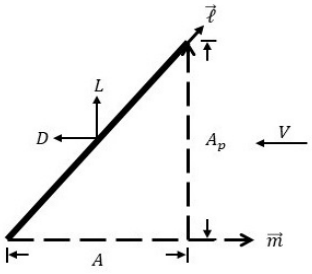

(a) Direction of Force if $\vec{\ell_i}\cdot\vec{m}_i \geq 0$

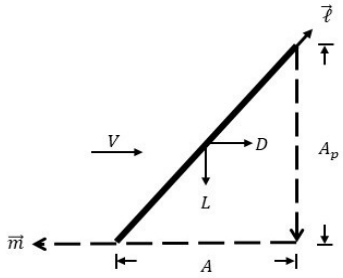

(b) Direction of Force if $\vec{\ell_i}\cdot\vec{m}_i < 0$

Figure 3: Direction of Force with Respect to Upstream Velocities.

The equilibrium equation of a subsea cable in catenary configuration for steady state cases in x-direction and y-direction can be given by Equations (8) and (9) respectively.

$$T_{x_i+1}\cos\alpha_{i+1} + T_{x_i}\cos\alpha_i + D_{x_i} + L_{x_i} = 0 \tag{8}$$

$$T_{y_i}\cos\beta_i + T_{y_i+1}\cos\beta_{i+1} + D_{y_i} + L_{y_i} + W\Delta s_i = 0 \tag{9}$$

where the angle calculation for the subsea cable elements $\alpha(s)$ and $\beta(s)$ were obtained by considering the dot product between vector $\vec{T}, \vec{i}$, and/or $\vec{j}$ as given in Equation (10).

$$\begin{aligned}
\vec{T}_i \cdot \vec{i} &= \left|\vec{T}_i\right| \left|\vec{i}\right| \cos\alpha_i, \\
\vec{T}_i \cdot \vec{j} &= \left|\vec{T}_i\right| \left|\vec{j}\right| \cos\beta_i, \\
\vec{T}_{i+1} \cdot \vec{i} &= \left|\vec{T}_{i+1}\right| \left|\vec{i}\right| \cos\alpha_{i+1}, \\
\vec{T}_{i+1} \cdot \vec{j} &= \left|\vec{T}_{i+1}\right| \left|\vec{j}\right| \cos\beta_{i+1}.
\end{aligned} \tag{10}$$

2.2.1 Boundary Conditions for Subsea Cable Problem in Catenary Configuration

Boundary conditions for subsea cable are important to the analysis process. In this paper, subsea cable were modelled by discretizing them into smaller elements as shown in Figure 4.

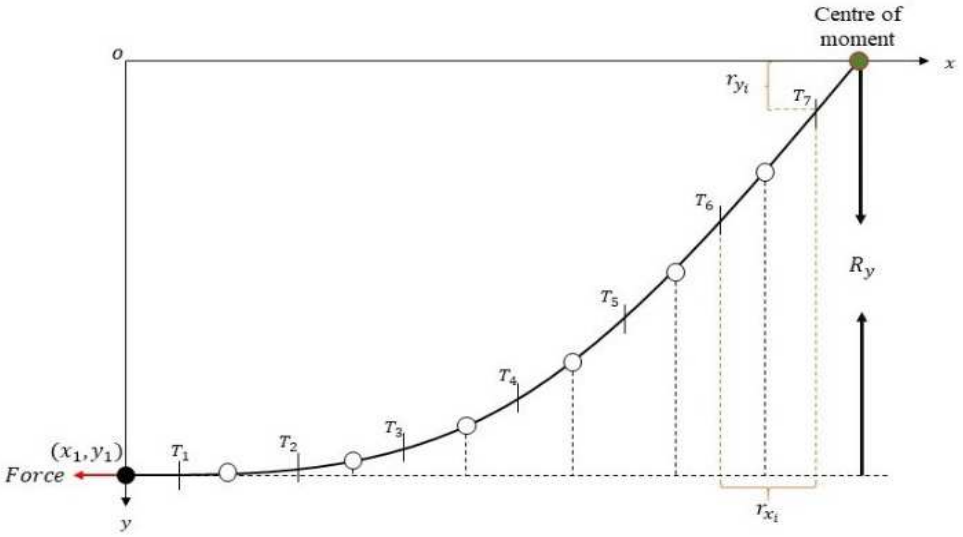

Figure 4: Subsea Cable Segment Division.

Based on Figure 4, (x_1, y_1) denotes TDP and the boundary condition at this point is based on a single moment of balance at the hanging point in the floating production vessel. This condition was considered as the subsea cable was assumed to have the properties of a rigid body element. The equilibrium force was considered in the clockwise and anti-clockwise direction using Equation (11) and (12), respectively.

Force in anti-clockwise rotation

$$W \cdot \Delta s_i \cdot r_{x_i} \tag{11}$$

Force in clockwise rotation

$$Force \cdot R_y \tag{12}$$

By combining both Equations (11) and (12), while considering drag and lift force, the equilibrium force at TDP from a single moment at sea surface node can be given as Equation (13).

$$\sum_{i=1}^{Ns} (W \cdot \Delta s_i \cdot r_{x_i} + D_{x_i} \cdot r_{y_i} + L_{y_i} \cdot r_{x_i}) = Force \cdot R_y,$$
$$Force = \frac{\sum_{i=1}^{Ns} (W \cdot \Delta s_i \cdot r_{x_i} + D_{x_i} \cdot r_{y_i} + L_{y_i} \cdot r_{x_i})}{R_y}. \tag{13}$$

Boundary condition at TDP can be said as equal to the *Force* obtained from a single moment at sea surface node ($T_1 = Force$). The boundary condition at the top node was obtained by projecting the force into the x-direction and y-direction. Total force at the top subsea cable node was described by Equations (14) and (15). $\bar{T}_1$ in equation (14) denotes the tension at TDP, which was calculated using the the total force based on a single moment at sea surface point.

$$T_{x_{Ns}} \cos \alpha_{Ns} = \bar{T}_1 \tag{14}$$

$$T_{y_{Ns}} \cos \beta_{Ns} = \sum_{2}^{Ns} (W \Delta s_i + L_{y_i}) \tag{15}$$

The input data in this study are tabulated as in Table 1. The parameter values were only for mathematical simulation and were not used as a benchmark for any actual problem.

Table 1: Input Data

Parameter	**Value**
Diameter of cable, d	0.023 m
Water depth, H	80 m
Density of cable, ρ_c	2888 kg/m^3
Density of water. ρ_w	1024.8103 kg/m^3
Cable weight in water, W	$\left(\pi \left(\frac{d}{2}\right)^2 (\rho_c - \rho_w)\, g\right) kg/ms^2$
Drag coefficient, C_D	1.2
Lift coefficient, C_L	0.024
Gravity, g	9.8 m/s^2
Relative velocity, V	1.2 m/s

2.3 Mathematical Model for Subsea Cables in a Lazy Wave Configuration

The second model was based on subsea cable in a lazy wave configuration. This model was developed to reduce slack formation and improve fatigue performance in subsea cable designs in catenary configuration. The model considered in this case illustrated in Figure 5.

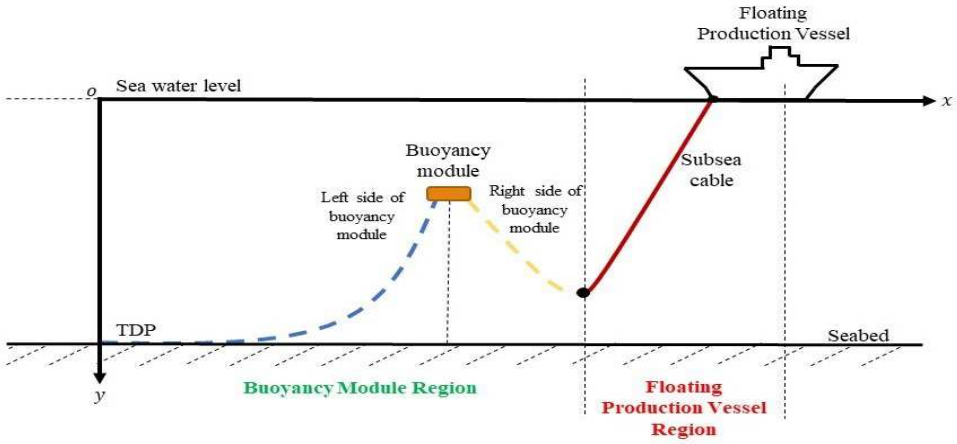

Figure 5: Illustration of Subsea Cables with Buoyancy Modules

This mathematical model for subsea cables was obtained by extending the formulation obtained for catenary problem. The equilibrium equation in y-direction was modified to consider the buoyancy force to the left and right region of the buoyancy module as illustrated in Figure 5. The equilibrium equation related to the x-direction was obtained directly from Equation (8). The equilibrium equation for subsea cables with buoyancy module in a two-dimensional steady state can be written in the x-direction and y-direction using Equation (16) and (17) respectively.

$x-$direction

$$T_{x_i+1}\cos\alpha_{i+1} + T_{x_i}\cos\alpha_i + D_{x_i} + L_{y_i} = 0 \tag{16}$$

$y-$direction

$$T_{y_i}\cos\beta_i + T_{y_i+1}\cos\beta_{i+1} + D_{y_i} + L_{y_i} + W\Delta s_i = 0$$

- Left element of the buoyancy module

$$T_i\cos\beta_i + \sum_{i=1}^{\substack{Left\ element\ of\\ buoyancy\ module}} (W\Delta s_i + L_{y_i}) = 0 \tag{17}$$

- Right element of the buoyancy module

$$T_{i+1}\cos\beta_{i+1} + \sum_{i=1}^{\substack{Right\ element\ of\\ buoyancy\ module}} (W\Delta s_i + L_{y_i}) = 0$$

- At the buoyancy module point

$$T_i\cos\beta_i + T_{i+1}\cos\beta_{i+1} - F_{bm} = 0$$

Note that the equilibrium equation at the buoyancy module point in Equation (17) was formulated to determine the buoyancy force of the buoyancy module. The buoyancy force of the buoyancy module was calculated considering the subsea cable element in which we proposed to implement the buoyancy module. The equation for calculating the buoyancy force of buoyancy module was written using Equation (18), where p denotes the desired buoyancy module weight percentage that will balance the buoyancy module in certain conditions while L denotes the length of the buoyancy module region.

$$\text{Buoyancy Force of the buoyancy module, } F_{bm} = L \cdot p \tag{18}$$

Boundary conditions for this problem were also based on the theory developed for the catenary configuration with slight modifications.

2.3.1 Boundary Conditions for Subsea Cable in Lazy Wave Configurations

The subsea cable configuration with a buoyancy module was created using an interpolation technique that discretized the subsea cable into N segments. For the boundary condition at TDP, Equation (13) was considered but the calculation was made based on the buoyancy module region illustrated in Figure 5 to produce Equation (19).

$$\begin{aligned} &\sum_{i=1}^{\substack{Buoyancy\\Node}} (W \cdot \Delta s_i \cdot r_{x_i} + D_{x_i} \cdot r_{y_i} + L_{y_i} \cdot r_{x_i}) = Force \cdot R_y, \\ &Force = \frac{\sum_{i=1}^{\substack{Buoyancy\\Node}} (W \cdot \Delta s_i \cdot r_{x_i} + D_{x_i} \cdot r_{y_i} + L_{y_i} \cdot r_{x_i})}{R_y}. \end{aligned} \tag{19}$$

Next, the boundary condition at the top node was calculated using Equations (14) and (15) but the calculations were only made on the floating production vessel region as shown in Figure 5. The equation for the boundary condition at the top node was calculated using Equations (20) and (21) in the x-direction and y-direction respectively.

$$T_{x_{Ns}} \cos \alpha_{Ns} = \bar{T}_1 \tag{20}$$

$$T_{y_{Ns}} \cos \beta_{Ns} = \sum_{\substack{Floating\\Production\\Vessel}}^{Ns} (W \Delta s_i + L_{y_i}) \tag{21}$$

The data considered for this case shown in Table 1. The effectiveness of the new formulated mathematical model in steady state condition was validated and compared with previous studies. A comparison between present and previous model was made using subsea cable tension analysis and cable configurations based on different parameters such as cable weight and cable diameter. The cable configuration of this study was similar to Yang *et al.* [13]. A comparison of subsea cable tension analysis between this study and previous study showed good agreement

for performance measurements such as cable diameter, water depth and current velocity. The formulated mathematical subsea cable model in a catenary configurations was then extended through the addition of buoyancy module. The results of both models are discussed in the next section.

3 Results and Discussion

The mathematical subsea cable model in this study was developed based on Yang *et al.* [13] and Han *et al.* [15]. The formulated model was updated with appropriate boundary conditions. To show the validity of the model, comparisons between the developed model and Yang *et al.* [13] were conducted as shown in the next section.

3.1 Comparison of Subsea Cable Tension with Past Study

The comparison of subsea cable tension analysis in this study and previous study was performed. The comparison showed good agreement for some performance measurements based on the input data given in Table 1. The comparison results are shown in Figure 6.

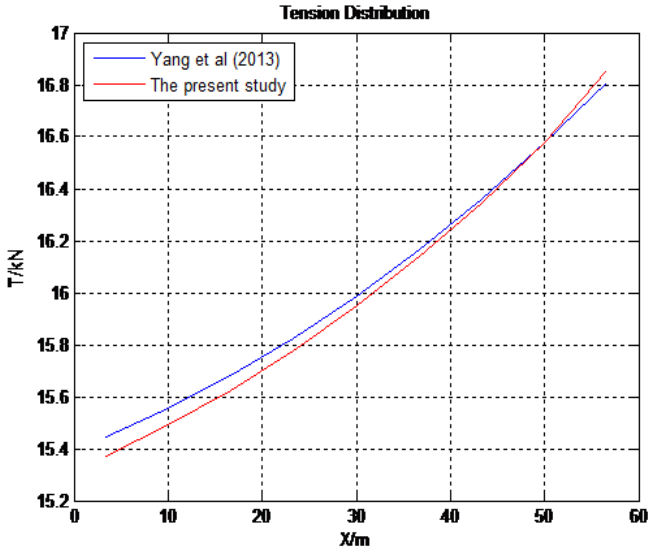

Figure 6: Tension Distribution Comparison for Past and Present Studies

As shown in Figure 6, the cable tension calculated in this study was smaller than Yang *et al.* [13] except for a very small portion around the sea surface. The top tension obtained in this study is larger than Yang *et al.* [13]. At the TDP the cable tension of this study was smaller than Yang *et al.* [13].

3.2 Tension Analysis of Subsea Cables in Catenary Configurations

Throughout the analyses, cable configurations is taken to be differ in their distance from the floating production vessel as illustrated in Figure 7. The objective function $f(T_1, T_2, \ldots, T_{Ns})$ was created to minimize subsea cable tension for analysis purposes based on the equilibrium

equation obtained in Equations (8) and (9) as well as boundary conditions of Equations (13) to (15) Table 2 shows the corresponding tensions in each cable element. The objective function was written as follows:

Let

$$netFy = \sum_{i=2}^{Ns} (W\Delta s_i + L_{y_i})$$

$x-$direction

$$f = f + \sum_{i=2}^{Ns-1} \left(T_{x_{i+1}} \cos\alpha_{x_{i+1}} + T_{x_i} \cos\alpha_{x_i} + D_{x_i} + L_{x_i}\right)^2$$

$y-$direction

$$f = f + \sum_{i=2}^{Ns-1} \left(T_{y_i} \cos\beta_{y_i} + T_{y_{i+1}} \cos\beta_{y_{i+1}} + +D_{y_i} + L_{y_i} + W\Delta s_i\right)^2$$

Boundary condition at TDP

$$f = f + \left(\bar{T_1} - Force\right)^2$$

Boundary condition at top node

$$f = f + \left(T_i \cos\alpha_i - \vec{T_1}\right)^2 + (T_i \cos\beta_i - netFy)^2$$

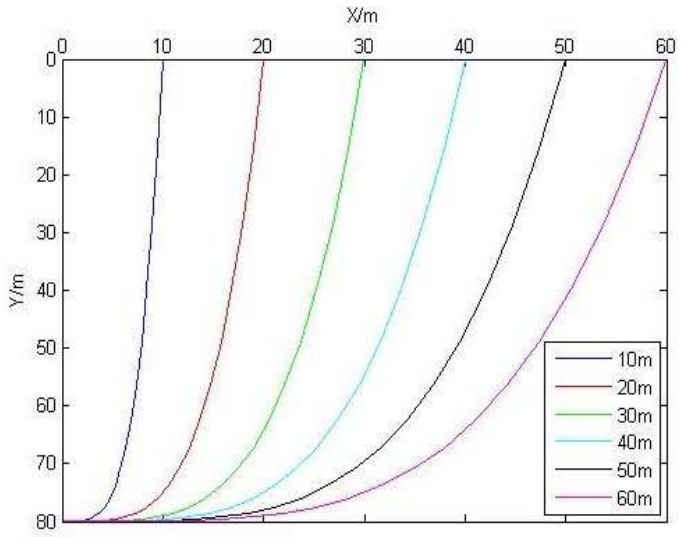

Figure 7: Cable Configuration of Different Distances from The Floating Production Vessel

Table 2: Tension Distribution Along Subsea Cables in Catenary Configurations (Starts from TDP)

Water depth (m)	80					
x-length (m)	10	20	30	40	50	60
Cable length (m)	83.2249	88.0197	93.6104	99.7614	106.3452	113.2799
Cable weight (N)	631.3675	667.7419	710.1545	756.8173	806.7638	859.3726
Tension distribution along the subsea cable (N)	16.7857	30.2317	44.6708	60.3627	77.4239	95.905
	24.1715	45.6149	66.9973	88.9452	111.7473	135.5564
	31.4381	60.8502	89.1665	117.3657	145.9060	175.0417
	38.4285	75.6349	110.8247	145.2455	179.5066	213.9573
	45.3028	89.7289	131.5610	172.0855	211.9972	251.7168
	52.6901	103.3053	151.1901	197.4889	242.8479	287.7005
	61.1201	117.0904	170.0429	221.4451	271.8017	321.4738
	70.6049	131.9018	188.9586	244.5071	299.1070	353.0263
	81.1180	148.0300	208.7753	267.5942	325.5233	382.8843
	93.0949	165.3509	229.8024	291.4442	351.9539	411.9217
	107.4282	183.9342	251.9354	316.2588	378.9480	440.9078
	125.3017	204.3681	275.2025	341.9342	406.5674	470.1588
	148.0801	227.7183	300.1260	368.5679	434.7391	499.6382
	177.2562	255.3804	327.7465	396.7601	463.6999	529.3681
	214.4303	288.9681	359.5013	427.6336	494.2127	559.7873
	261.3033	330.2468	397.1006	462.7235	527.5530	591.8752
	319.6746	381.1018	442.4432	503.8571	565.3982	627.101
	391.4430	443.5232	497.5687	553.0681	609.7171	667.3144
	478.6078	519.6002	564.6317	612.5426	662.6870	714.6419

For each configuration, tension increases from TDP to its maximum value at the hanging point. This is due to a gravitational effect in which the cable element at the TDP is resting horizontally on the seabed while the cable elements near the hanging point does not have support and has to withstand the weight of the cables below. For the cable length in the x-direction of 60m, it can be seen clearly in Table 2 that the tension distribution for the subsea cable reached more than 500N. Apart from this, the longer the cable, the higher the tension at hanging point for each cable. In order to reduce cable tension, a support is needed such as a buoyancy module which will create a lazy wave configuration that will reduce the extreme stresses and fatigue of the subsea cable to within an acceptable limit.

3.3 Tension Analysis of Subsea Cables for Lazy Wave Configurations

The tension analysis of subsea cables with a lazy wave configuration problem were based on Equations (16) and (17). The cable configuration for this case was created based on several different buoyancy module distances from the seabed (30m, 40m and 50m) and from the floating production vessel (20m, 30m and 40m). Note that the x-distance of the cable length was fixed at 60m, so it could be compared to the last column of Table 2 for subsea cable configurations without a buoyancy module. The objective function $f(T_1, T_2, \ldots, T_{Ns})$ was created based on the equilibrium equation obtained in Equations (16), (17), (19), (20) and (21).

3.3.1 Tension Analysis of Subsea Cables with Buoyancy Module 30m from Seabed

The buoyancy module was installed 30m from the seabed illustrated in Figure 8, with different distances from the floating production vessel of 20m, 30m and 40m respectively.

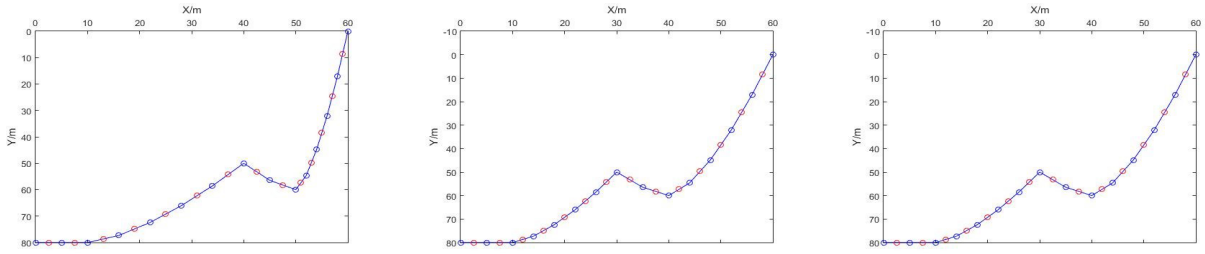

(a) (b) (c)

Figure 8: Cable Configuration with Buoyancy Module 30m from Seabed (a)20m, (b)30m and (c)40m distance from floating Production Vessel

Table 3: Tension Distribution Along Subsea Cables With Buoyancy Module 30m from Seabed With Varying Distances from the Floating Production Vessel.

Distance from Production floating vessel (m)	**20**	**30**	**40**
Cable Length, L (m)	**128.3809**	**124.6065**	**122.7833**
Cable Weight, ω (N)	**973.9330**	**945.2994**	**931.4683**
Length of buoyancy module region, Lbm (m)	**57.4130**	**50.8960**	**52.1399**
Percentage of buoyancy force of buoyancy module from cable weight (%)	**44.7208**	**40.8454**	**42.465**
Buoyancy force of buoyancy module, Fbm (N)	**435.5506**	**386.1113**	**395.5480**
Tension distribution along subsea cable	116.0901	128.5787	129.6231
	182.6476	157.7708	133.2669
	272.9907	225.1328	183.6846
	346.7153	290.1963	246.8085
	403.4473	346.9344	305.5861
	449.5396	398.2311	361.9553
	421.1755	369.7982	352.9194
	116.7688	76.6283	77.9900
	10.3627	11.2398	31.6236
	66.9689	90.3609	111.7599
	141.7811	180.4623	207.7665
	226.0713	263.4413	289.6859
	320.7865	347.6782	368.6213
	425.5860	435.5577	448.1036

Table 3 shows the corresponding tensions in each cable element. The buoyancy module point was outlined by a black color in Table 3. All the results had an appropriate tension distribution along the subsea cable that did not exceed the critical value of 500N.

3.3.2 Tension Analysis of Subsea Cables with Buoyancy Module 40m from Seabed

This section discusses on the results for the buoyancy module 40m from the seabed which are shown in Figure 9 with a distance from the floating production vessel of 20m, 30m and 40m respectively.

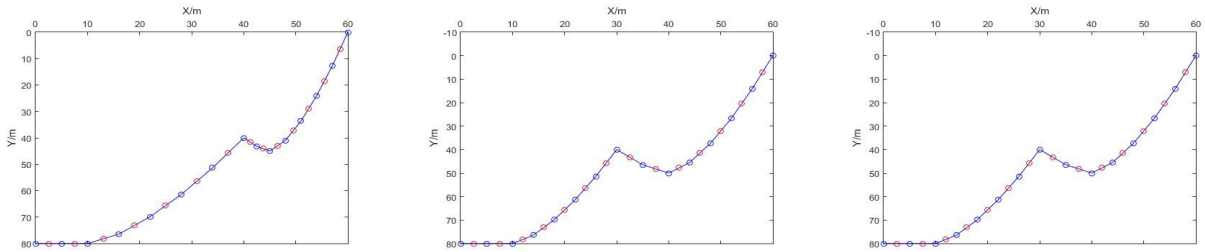

(a) (b) (c)

Figure 9: Cable Configuration with Buoyancy Module 40m from Seabed (a)20m, (b)30m and (c)40m distance from floating Production Vessel.

Table 4: Tension Distribution Along Subsea Cable With Buoyancy Module 40m from Seabed With Varying Distances from Floating Production Vessel

Distance from Production floating vessel (m)	**20**	**30**	**40**
Cable Length, L (m)	**115.7260**	**123.9171**	**129.4244**
Cable Weight, ω (N)	**877.9295**	**940.0698**	**981.8493**
Length of buoyancy module region, Lbm (m)	**57.9431**	**59.5587**	**65.3475**
Percentage of buoyancy force of buoyancy module from cable weight (%)	**50.0693**	**48.0633**	**50.4909**
Buoyancy force of buoyancy module, Fbm (N)	**439.5732**	**451.8286**	**495.7445**
Tension distribution along subsea cable	134.5136	123.8149	129.4996
	192.3757	146.3506	132.0996
	291.3476	226.5843	195.5351
	379.6133	310.7893	277.8992
	452.3928	388.3120	355.8800
	515.7113	462.4791	432.5333
	460.6796	439.7050	428.7612
	41.7102	47.4190	86.5045
	9.2771	5.6127	10.9831
	74.5028	78.8936	81.4881
	142.5091	161.6504	180.4553
	205.4149	233.3620	262.5427
	269.2971	303.2451	340.0879
	335.9230	374.0892	416.8582

The buoyancy module point was outlined using a black color in Table 4. The cable configuration with buoyancy module position of 30m or 40m from the floating production vessel also had an appropriate tension distribution along the subsea cable less than 500N.

3.3.3 Tension Analysis of Subsea Cable with Buoyancy Module 50m from Seabed

This section discusses the results for the buoyancy module 50m from the seabed as shown in Figure 10 with different distances from the floating production vessel of 20m, 30m and 40m respectively.

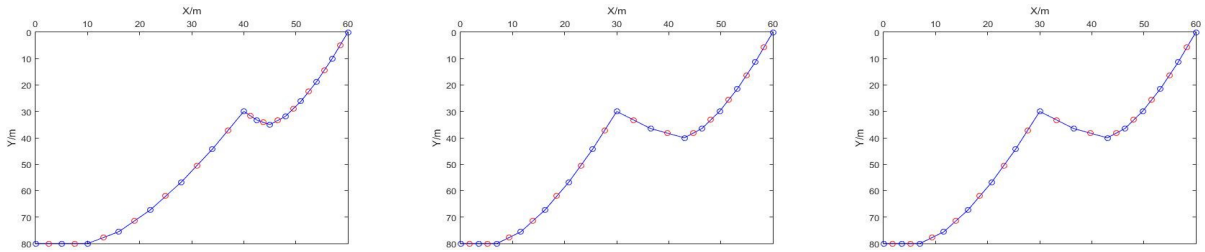

(a) (b) (c)

Figure 10: Cable Configuration with Buoyancy Module 50m from Seabed (a)20m, (b)30m and (c)40m distance from floating Production Vessel.

Table 5: Tension Distribution Along Subsea Cable With Buoyancy Module of 50m from Seabed With Varying Distances from Floating Production Vessel

Distance from Production floating vessel (m)	**20**	**30**	**40**
Cable Length, L (m)	**114.7503**	**123.1169**	**129.8866**
Cable Weight, ω (N)	**870.5274**	**933.9989**	**985.3554**
Length of buoyancy module region, Lbm (m)	**66.2816**	**72.2137**	**74.7230**
Percentage of buoyancy force of buoyancy module from cable weight (%)	**57.7616**	**58.6546**	**57.5294**
Buoyancy force of buoyancy module, Fbm (N)	**502.8306**	**547.8333**	**566.8691**
Tension distribution along subsea cable	133.5274	118.2690	123.9169
	186.9246	146.9233	198.3902
	299.7340	244.8775	295.0623
	407.5620	350.3030	389.8611
	501.6933	448.0700	486.1186
	588.2340	542.8555	492.2768
	529.1723	526.7026	68.9125
	12.2269	34.6975	34.5218
	4.1796	3.9363	10.6727
	64.8008	64.4133	88.7526
	125.6519	135.3596	173.1213
	177.6867	196.0328	238.3586
	227.6672	254.4308	296.3969
	277.7345	313.0019	351.1620

The buoyancy module point was outlined by using a black color in Table 5. Based on the three models, only cable configurations with a buoyancy module position 40m from the floating production vessel had an appropriate tension distribution along the subsea cable that was less than 500N.

4 Conclusion and Recommendations

Mathematical models of subsea cable for both catenary and lazy wave configurations were generated with assumption that velocity was constant, the seabed was flat, and the effects of wind and waves were insignificant. Two solutions were presented in this paper: tension analysis for subsea cables without buoyancy modules (catenary configuration), and tension analysis for subsea cables with buoyancy modules (lazy wave configuration). Both solutions used the same unconstrained minimization approach. It can be seen clearly in the report that the tension distribution for subsea cables in the catenary configuration was greater than 500N, which will cause a large hang-off load at the floating production vessel.

Buoyancy modules were installed in a suitable section of the catenary cable shape, forming a lazy wave configuration that reduced the tension of the subsea cable at the floating production vessel. From the nine different buoyancy module positions, the best buoyancy module position was 30m from the seabed and 30m from the vessel because its tension distribution was the lowest and was below the acceptable limit of 500N. Moreover, the buoyancy force used for this configuration was also smaller than other configurations. The proposed buoyancy module should have a buoyancy force percentage within 40% of the total subsea cable weight.

In future research, this study suggests researchers to investigate more reliable lazy wave configurations since different shapes will produce different amounts of tension along the subsea cable. Subsea cable configurations should be developed based on different criteria such as different buoyancy force, buoyancy module distance from the seabed, and buoyancy module distances from the floating production vessel.

Acknowledgement

The authors would like to express gratitude to the Ministry of Higher Education Malaysia for their financial support through MyBrainSc Scholarship throughout study period.

References

[1] Zajac, E. Dynamics and kinematics of the laying and recovery of submarine cable. *The Bell System Technical Journal*. 1957. 36(5): 1129-1207.

[2] Yoshizawa, N. and Yabuta, T. Study on submarine cable tension during laying. *IEEE Journal of Oceanic Engineering*. 1983. 8(4): 293-299.

[3] Burgess, J. Modelling of undersea cable installation with a finite difference method. *Paper presented at the The First International Offshore and Polar Engineering Conference*. 1991.

[4] Patel, M. and Vaz, M. The transient behaviour of marine cables being laid—the two-dimensional problem. *Applied Ocean Research*. 1995. 17(4): 245-258.

[5] Vaz, M., Witz, J. and Patel, M. Three dimensional transient analysis of the installation of marine cables. *Acta Mechanica*. 1997. 124(1-4): 1-26.

[6] Vaz, M. and Patel, M. Three-dimensional behaviour of elastic marine cables in sheared currents. *Applied Ocean Research*. 2000. 22(1): 45-53.

[7] Chucheepsakul, S., Srinil, N. and Petchpeart, P. A variational approach for three-dimensional model of extensible marine cables with specified top tension. *Applied Mathematical Modelling*. 2003. 27(10): 781-803.

[8] Wang, F., Huang, G.-l. and Deng, D.-h. Steady state analysis of towed marine cables. *Journal of Shangsai Jiatong University (Science)* 2008. 13(2): 239-244.

[9] Wang, Y., Bian, X., Zhang, X. and Xie, W. A study on the influence of cable tension on the movement of cable laying ship. *Paper presented at the OCEANS 2010 MTS/IEEE SEATTLE*. 2010.

[10] Yang, N. and Jeng, D.-S. Three-dimensional Analysis of Elastic Marine Cable during Laying. *Paper presented at the The Eleventh ISOPE Pacific/Asia Offshore Mechanics Symposium*. 2014.

[11] Dreyer, T. and Van Vuuren, J. H. A comparison between continuous and discrete modelling of cables with bending stiffness. *Applied Mathematical Modelling*. 1999. 23(7): 527-541.

[12] Park, H., Jung, D. and Koterayama, W. A numerical and experimental study on dynamics of a towed low tension cable. *Applied Ocean Research*. 2003. 5(5): 289-299.

[13] Howison, S. *Practical Applied Mathematics: Modelling, Analysis, Approximation*. Cambridge University Press. 2005.

[14] Yang, N., Jeng, D. and Zhou, X. Tension analysis of submarine cables during laying operations. *Open Civ. Eng. J.* 2013. 7(1): 282-291.

[15] Han, H., Li, X. and Zhou, H.-S. 3D mathematical model and numerical simulation for laying marine cable along prescribed trajectory on seabed. *Applied Mathematical Modelling* 2018. 60: 94-111.

[16] Abidin, A. R. Z., Mustafa, S., Aziz, Z. A. and Ismail, K. Subsea Cable Laying Problem. *Matematika*. 2018. 34(2): 173-186.

[17] Wang, J., Duan, M., Fan, J. and Liu, Y. Static equilibrium configuration of deepwater steel lazy-wave riser. *Paper presented at the The Twenty-third International Offshore and Polar Engineering Conference*. 2013.

[18] Wang, J. and Duan, M. A nonlinear model for deepwater steel lazy-wave riser configuration with ocean current and internal flow. *Ocean Engineering*. 2015. 94: 155-162.